ACCURATE TOF CAMERA DATA FOR ROBOTIC APPLICATIONS

Fuchs S. and Suppa M. - DLR, Institute of Robotics and Mechatronics
{stefan.fuchs, michael.suppa}@dlr.de

ICVSS 2010
Registration and Video Analysis

Abstract

ToF cameras provide range and intensity images at video frame rate independent of textures or illumination. By now, ToF sensors are available with a resolution of 204×204 pixels allowing for conventional computer vision algorithms and opening up new possibilities. The frame rate enables real-time applications, e.g ego-motion-estimation or visual servoing. Admittedly, the complex error characteristic of ToF cameras constrains their spread.
Using the example of object localization and ego-motion-estimation this poster describes two approaches dealing with this errors.

ToF Camera Calibration

Non harmonic properties of the optical signal, i.e. not perfectly sinusoidal signal, generate a distance-related error. In [1] we described a calibration method, which identifies this error component and approximates it by a spline. Using amplitude and depth images of a checkerboard from different points of views, a common photogrammetric intrinsic and extrinsic calibration is performed initially. Then, the distance-related error is identified in a depth calibration step. As a result, for distance measurements an overall mean accuracy of $3\ \mathrm{mm}$ is achievable.

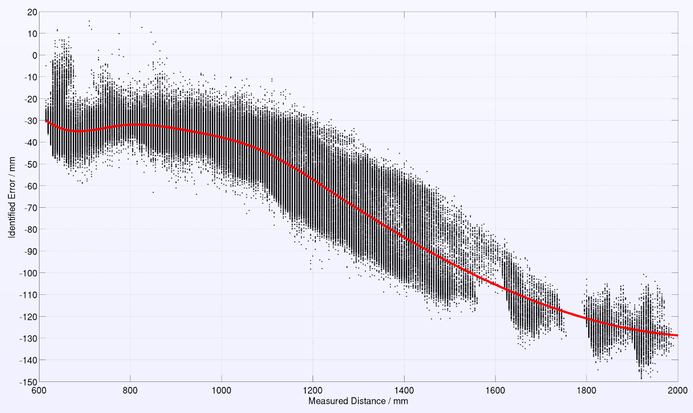

Object Localization

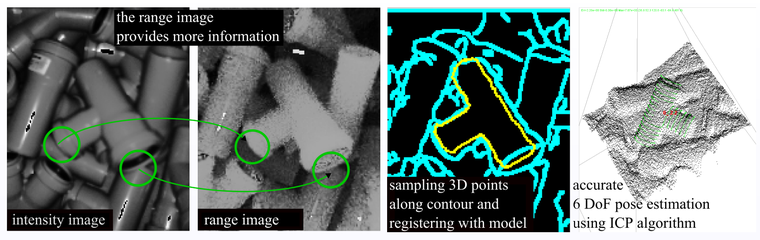

The range images allow for computer vision algorithms when there is less information in the intensity images, e.g. due to the lack of textures. Along recognized contours, 3D points are created. Hence, the metric dimension of the recognized structure is measurable. Thus, the search space and the computational efforts of object recognition or localization algorithms are reduced. A recognized object is localized by sampling a number of rotations at the barycenter and registering these with a model contour. Pose Refining with an ICP algorithm yields an accuracy of $7\ \mathrm{mm}$ and $3\ °$.

References

[1] Fuchs S., Hirzinger, G., Extrinsic and Depth Calibration of Time-of-Flight Cameras, in *In Proceedings of the CVPR*, 2008

[2] May, S., Fuchs, S., Droeschel, D., Holz, D., Nuechter, A., Robust 3D-Mapping with Time-of-Flight Cameras, in *Proceedings of the IROS*, 2009

ToF Camera Measurement Principle

The ToF camera emits sinusoidal modulated **N**ear-**I**nfra**R**ed (NIR) light. The NIR light is reflected by the observed scene and projected onto a CMOS or CMOS/CCD pixel matrix. The distances and intensities are computed within every pixel. Thus, the ToF camera provides range and intensity images at video frame rate independent of texture and illumination. In conjunction with a small-sized and handy design, ToF sensors are a promising alternative to laser-scanners and stereo camera systems.
ToF cameras are not widespread yet, despite their suitability for a wide range of applications that require 2D/3D information, such as object detection and localization, surveillance tasks or collision avoidance in mobile robotics. The reason for that is primarily the complex error characteristic of the ToF camera.
Besides the known intrinsic systematic errors coming from the camera optics, there are two critical ToF camera specific errors:

Distance related error, and

Multi**P**ath **I**nterference (MPI).

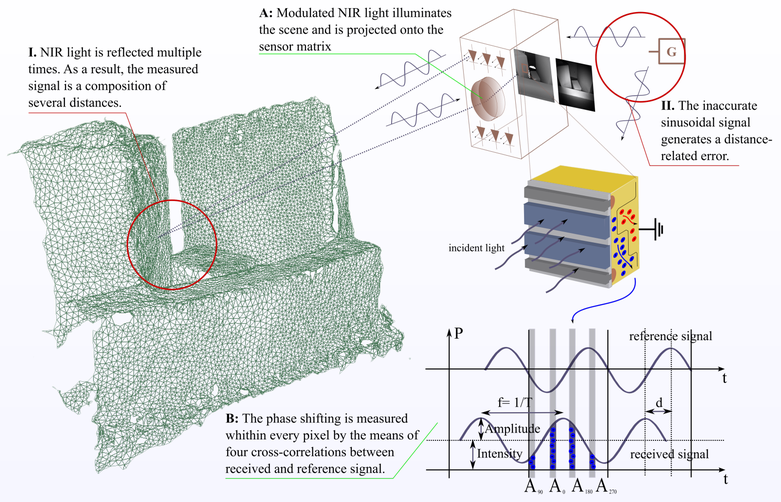

Schematic illustration of the measurement principle and its basic error sources. The distance-related error arises inside the camera, whereas the MPI is defined by the scene configuration.

Multipath Interference Model

Multipath interference can influence the ToF camera measurements by several centimeters. In order to mitigate the impact of the MPI we formulate a multipath model. Therefor, we introduce two simplifications:

1. light source and surfaces are Lambertian Emitters
2. the luster cone is congruent with the camera's fov

In the right diagram L illuminates the whole scene. Beam A irradiates $\mathbf{p}$ and the NIR light is reflected. The received amplitude $a^{in}_{\mathbf{p}}$ and phase $\Delta\phi$, which is proportional with the covered distance $2\|\mathbf{p}\|$, are denoted in a complex way

$$s(\mathbf{p}) = a^{in}_{\mathbf{p}} e^{j\Delta\phi(2\|\mathbf{p}\|)} \quad . \tag{1}$$

At the same time, a 2nd beam B irradiates the surface at $\mathbf{q}$, which reflects incident light to $\mathbf{p}$, as illustrated by the beam C. So, beam B contributes via $\mathbf{q}$

$$s(\mathbf{q})^+ = a^+_{\mathbf{q}} e^{j\Delta\phi(\|\mathbf{p}\|+\|\mathbf{q}\|+\|\mathbf{q}-\mathbf{p}\|)} \tag{2}$$

to $s(\mathbf{p})$. As a result, the measured signal $\hat{s}(\mathbf{p})$ is a composition of

$$\hat{s}(\mathbf{p}) = s(\mathbf{p}) + s(\mathbf{q})^+ \quad . \tag{3}$$

The key to MPI simulation is estimating the the magnitude $a^+_{\mathbf{q}}$ of all additional reflections. In order to compensate the error a weighted sum of all additional distance parts and phasors respectively is computed and subtracted from the measured distances.

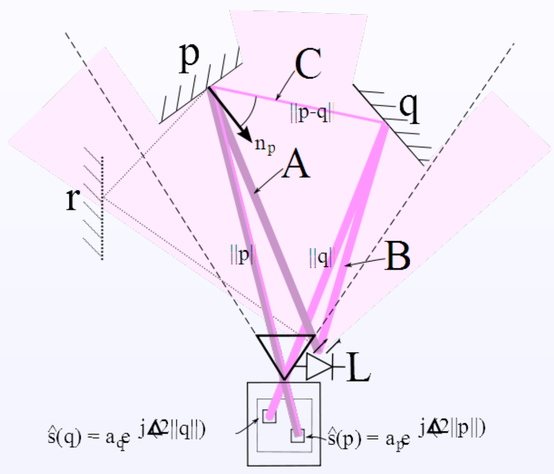

The diagram illustrates a luster cone not being congruent with the camera's field of view (dashed line). In this case, the unseen surface $\mathbf{r}$ also influences the measurement (dotted line).

Ego-Motion-Estimation

Simultaneous localization and mapping is of great interest in mobile robotic applications. In this context, the ToF camera was mounted on an industrial robot and moved while capturing a simple scene configuration. The ToF camera's ego-motion was estimated by applying an ICP algorithm (see [2]).

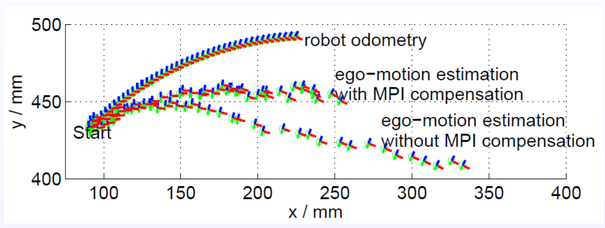

The measured and estimated trajectories are plotted in the diagram. The ego-motion-estimation without MPI compensation shows a large deviation. Applying the MPI compensation reduces the localization error from $140\ \mathrm{mm}$ to $60\ \mathrm{mm}$ and from $2.5\ °$ to $0.5\ °$.

MPI Compensation

The left diagram plots the bird's eye view of a corner located $1\ \mathrm{m}$ in front of the camera. The green points are measured with a laser scanner system. The red points are captured with the ToF camera and affected by MPI.

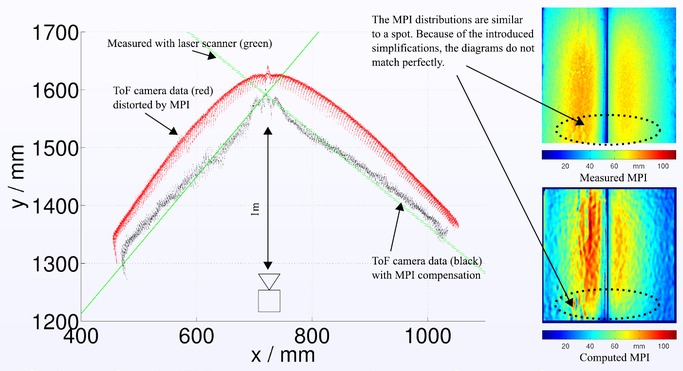

Applying the MPI compensation reduces the root mean squared error from $57\ \mathrm{mm}$ to $17\ \mathrm{mm}$ (black). The right diagrams illustrate the measured (top) and computed MPI related error (bottom) in this corner scene.